A Customizable Aptamer Transducer Network Designed for Feed-Forward Coupling

*Tim Hachigian [a], Drew Lysne [a], Elton Graugnard [a], and Jeunghoon Lee [a,b] **

[a] Micron School of Materials Science and Engineering

Boise State University, 1910 University Dr., Boise, ID, 83725, USA.

[b] Department of Chemistry and Biochemistry

Boise State University, 1910 University Dr., Boise, ID, 83725, USA.

*To whom correspondence should be addressed

Abstract

Solution based biosensors that utilize aptamers have been engineered in a variety of formats to detect a range of analytes for both medical and environmental applications. However, since aptamers have fixed base sequences, incorporation of aptamers into DNA strand displacement networks for feed-forward signal amplification and processing requires significant redesign of downstream DNA reaction networks. We designed a novel aptamer transduction network that releases customizable output domains, which can then be used to initiate downstream strand displacement reaction networks without any sequence redesign of the downstream reaction networks. In our aptamer transducer, aptamer input domains are independent of output domains within the same DNA complex and are reacted with a fuel strand after aptamer-ligand binding. Aptamer transducers were designed to react with two fluorescence dye-labeled reporter complexes to show the customizability of the output domains, as well as being used as feed-forward inputs to two previously studied catalytic reaction networks, which can be used as amplifiers. Through our study we show both successful customizability and feed-forward capability of our aptamer transducers.

Introduction

Aptamers are single stranded nucleic acid sequences that bind selectively to a target ligand with high affinity. Identification of aptamers occurs through systematic evolution of ligands by exponential enrichment (SELEX), which has identified several hundred sequences to date.[1–6] A duplexed aptamer is formed by hybridizing an aptamer with a short complementary sequence known as an aptamer complementary element.[7,8] Duplexed aptamers that release an aptamer complementary element upon biomolecular interaction with the sensing target have been used as sensing elements in novel aptamer biosensors.[1,2] Biosensors utilizing such duplexed aptamers have been developed in a variety of formats, including solution FRET, surface FRET, solution fluorescence, surface fluorescence, electrochemistry, nucleic acid circuits, colorimetry, and nanoparticle FRET.[3,5–22] While these approaches all offer biosensing capability, biosensors that incorporate nucleic acid circuits in particular, offer unique advantages because of their natural compatibility with DNA reaction networks capable of signal processing, signal amplification, and logic operations.[23,24] Aptamer Reaction Networks (ARNs) are DNA reaction networks that incorporate an aptamer as an element to trigger a nucleic acid circuit. The usefulness of an ARN lies in its ability to transduce a biomolecular input of target analytes into a nucleic acid signal.[18,25,26] When integrated with simple and inexpensive detection technologies, ARNs could one day become a potential replacement for assays that require more intensive labor or expensive equipment.[26] Investigation of more sensitive and well-designed ARN circuit components is critical for the development of sensing technologies for medical diagnostic and environmental applications.

Because an ARN produces a DNA output, it is capable of triggering further logic operations and signal amplification by downstream DNA reaction networks through feed forward signaling.[27] This feed forward capability has made reaction networks a noted area of interest in aptamer biosensing.[1,13,15,18,28] For example,

Cheng et al. demonstrated the coupling of the adenosine aptamer into a feed forward catalytic reaction network employing both target inhibited and target triggered approaches to amplify the detection of adenosine.[15,28] Furthermore, they utilized the aptamer strand or its complement to trigger a catalytic cycle in their network design. In this example, however, the ARN produced an output that is dependent on the aptamer sequence.[15,28] As a result, these networks require significant sequence redesign of downstream DNA reaction networks for their intended function. Zhu et al., for example, developed an aptamer transduction unit based on a three-way junction that could translate a target-inhibited aptamer signal into an arbitrary output. The network's feed forward capability, however, was not demonstrated.[21] Other approaches toward developing a universal aptamer biosensor lack a transduction step and operate as labeled molecular beacons or as simple direct colorimetric devices.[7,13,16,17,19,25]

While feed forward functionality has been considered by some groups,[1,13,15,18,28] the community has focused more on modifications to increase the sensitivity of ARNs. Since aptamer biosensors are generally limited by the inherent aptamer-ligand binding affinity (K_d), approaches for designing more sensitive detectors depend on modifying an aptamer strand because its effective binding affinity ($K_{d,eff}$) can be improved with targeted alterations to its base sequence, including hybridization of complementary elements.[1–3,7–14,14–23,25,26,28–34] For example, many studies have aimed to optimize the adenosine aptamer effective binding affinity ($K_{d,eff}$) by manipulating the location of the aptamer sequence in their biosensor designs or by direct aptamer sequence alterations such as truncation and mutation.[25,35] These studies have shown that even greater binding affinities can be achieved for many of the known aptamers using such modifications. Screening of novel aptamers through SELEX is another route for identifying selective aptamer sequences that yield greater sensitivities toward the same target.[31] As novel and more sensitive aptamers are developed and discovered, general approaches for incorporating them into modular ARNs will be critical for the creation of biosensors with improved functionalities and performances.

While many studies have dealt with increasing aptamer sensitivity, relatively few studies have attempted to incorporate such aptamers into two-layer feed forward networks.[13,28] A feed-forward DNA reaction network is composed of multiple consecutive reaction networks in which the output of the first network functions as the input for the subsequent network. Using feed forward functionality allows for greater modularity between reaction networks, since different reaction networks can be chained together to achieve multi-functionality. For example, an ARN can be first used for biosensing and then can be chained to a catalytic network for signal amplification. Using an ARN in a feedforward network presents a unique challenge since the output of an ARN is dependent on the base sequence of the aptamer, which in turn requires a redesign of a subsequent network. Therefore, there is significant motivation to design ARNs that can transduce a molecular signal from the target into multiple DNA outputs without the need for significant domain level redesigns of downstream networks.

In this work, we introduce an *Aptamer Transducer (AT)* as a non-enzymatic, modular, and customizable ARN that can be implemented in two-layer feedforward reaction networks. Using the well-known Huizenga & Stozak adenosine aptamer, we have designed and tested a practical biosensing platform that can fully transduce an adenosine signal into arbitrary DNA outputs based on a structure-switching aptamer design, where the AT's output domain is not dependent on the sequence of the adenosine aptamer.[30] This design modularity was accomplished by separating the aptamer input domain from the output domain, which is sequestered in a hairpin region of the AT complex. Incorporating an additional fuel strand into the AT design allows for the release of the output strand upon successful toehold mediated DNA strand displacement. Two dye and quencher labeled reporter complexes, differing in sequence, were used to show that the AT can successfully output differing signals. To further demonstrate the ATs customizability, we incorporated the AT with two catalytic amplification networks – an entropy-driven catalytic network developed by Zhang et al.[23] and a 3-arm catalytic amplification network developed by Kotani et al.[24]

Results and Discussion

As illustrated in Figure 1A, two critical regions for the functionality of AT are the aptamer input region (blue box) and the DNA Output region (brown box). The 6-nt long aptamer complement domain **τ'** is duplexed to the aptamer input domain (**α**), forming the structure-switching element of the sensor. Upon aptamer-ligand binding, the **τ'** domain dehybridizes from the aptamer to act as a toehold for an invading fuel strand. DNA strand displacement is initiated once the **τ'** domain of the AT and **τ** domain of the fuel hybridize, initiating 3-way branch migration to replace $\boldsymbol{\beta_1}$ of the output strand. DNA strand displacement continues with 4-way branch migration through the **μ** domain. Finally, the 3-way branch migration through the $\boldsymbol{\beta_2}$ domain releases the output signal from the backbone of the AT, which makes available **λ** and **μ** domains as a ssDNA signal for downstream reactions. The **μ'** was added to the fuel strand to suppress the cross-talk between **μ** domain of the fuel and **μ'** domain of the reporter complex.

Overall, the AT is analogous to an AND gate that requires both the ligand and the fuel as inputs to transduce a ligand signal into a ssDNA output. Using a fuel strand in the design allowed us to keep the aptamer and output sequences independent in the AT complex. Additionally, the reaction benefits from using a fuel, since the AT reaction becomes more irreversible. Once fuel has reacted with the substrate, it is much less likely for the original AT to reform, and therefore any output domains that are released remain available for downstream reactions. Since the **λ** and **μ** domains are independent of the aptamer sequence, their domain level sequences can be customized toward any desired output. To support this claim, multiple reporter probes and ATs differing in output sequences have been designed and tested using the same aptamer input region.

Integration of AT with unique Reporters

The adenosine binding DNA aptamer was chosen as the **α** domain, since it has been a well-studied aptamer in previous ARNs, providing a good basis for comparing sensitivity.[16,18,21,22,26,31,32] The reaction of the AT, as illustrated in Figure 1A, proceeds with the binding of adenosine with the **α** domain, which has been shown to have two possible binding sites, freeing the **τ'** toehold.[16,18,21,22,26,31,32] Next, the fuel strand releases the output strand producing a waste 1 complex and frees **λ** and **μ** domains. These output domains can initiate other downstream reaction networks or reporters. Since **λ** and **μ** domains are independent of the **α** domain, they can be custom-designed to suit the input required for subsequent DNA reaction networks. To test the customizability of **λ** and **μ** domains, the AT was first integrated with duplexed dye-quencher reporters.

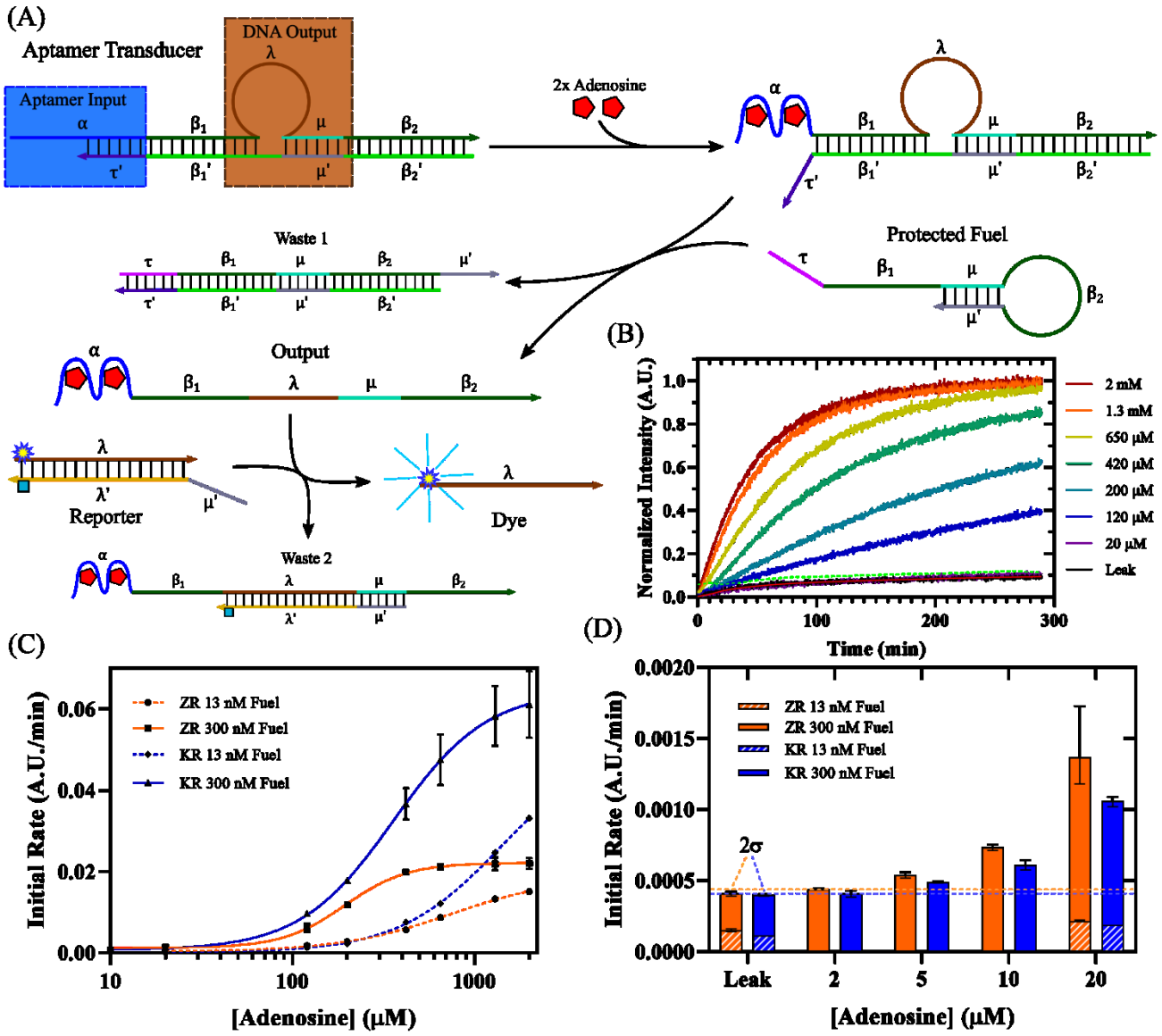

Figure 1: (A) Reaction schematics of the AT binding to adenosine, releasing ssDNA output, and reacting with a reporter complex. The structure switching aptamer input region is shown in the blue box and the ssDNA output region is shown in the brown box. (B) Fluorescence intensity normalized by the maximum intensity of the 2 mM adenosine trace shows the kinetic behavior of the AT reacting with a ZR reporter as initiated by 20 µM – 2 mM adenosine, using 13 nM protected fuel, over 300 minutes. Calculated 2σ of the leakage trace (green dash) and the leakage moving average (red line) are also shown. (C) Initial rates of the AT reacting with ZR and KR reporters using both 13 nM and 300 nM AT fuel (10 nM AT complex, 20 nM Reporter) in 1×TE 25 mM Mg^{2+} (D) Initial rates of the AT reacting with ZR and KR using low concentrations of adenosine 2-20 µM compared to the AT leakage rate. Initial rates above 2σ of the leak are considered detected.

Two distinct TET/Iowa Black labeled reporters, whose sequences were derived from two amplification networks reported by Zhang et al. (ZR) and Kotani et al. (KR), were used to track the concentration of the output signal strand and overall reaction kinetics.[23,24] These two reporters were chosen because they have previously been shown as reliable reporters for their respective amplification reaction networks. Upon dehybridization of the reporter by the output strand, the dye and the quencher are separated, reducing the fluorescence quenching and increasing the TET dye's fluorescence signal that can be continuously monitored. In addition, two unique reporter

complexes were used to validate the modularity of the AT output domains. By showing that the AT can accommodate two unique reporter sequences selected from previous network designs, we validate that the AT can output arbitrary DNA sequences through redesign of only two domains and demonstrate the AT's universal signal transduction capability. In addition to modularity, initial testing with simple reporters allowed us to characterize fundamental AT network performance metrics such as reaction rates, network leakage, and detection sensitivity without convoluting the system with additional reaction steps. The AT's ability to accommodate customized outputs is further supported by showing that different output domain lengths can be incorporated, since a universal transduction platform should not be constrained by output domain lengths or specific DNA sequences.

ZR and KR were mixed with their respective AT and were triggered by adenosine concentrations ranging from 2 μM to 2 mM. The limit of detection for adenosine sensing was determined by calculating the second standard deviation (2σ) of the leakage kinetic trace in each system, which describes the system's overall reaction without the presence of adenosine. Any signal that exceeds 2σ was considered sensed with 95% confidence limits above the system noise.[28,36] Representative kinetic traces for the AT reacting with the ZR is shown in Figure 1B. Over 300 minutes, the ATs integrated with ZR and KR were able to resolve varying adenosine concentrations. Initial reaction rates were determined by linearly fitting fluorescence intensity versus time traces for each adenosine concentration, within the first 30 minutes, using ATs reacted with ZR and KR and two fuel concentrations (13 nM and 300 nM, Figure 1C and 1D), the slope that represent the initial reaction rates were used as a metric to compare reaction kinetics for each system. At adenosine concentrations above 120 μM, KR reacts more quickly than ZR because of its longer toehold (**μ'** domain) and greater GC content, which is 7 nt for ZR with 28% GC content and 10 nt for KR with 50% GC content. A higher initial reaction rate for KR is expected since longer toeholds with greater GC content provide favorable energetics for initial toehold binding and a greater barrier to spontaneous toehold dissociation.[30,37] At low adenosine concentrations (20 μM and below, Figure 1D) ZR showed slightly faster reaction rates although both systems were not able to detect 2 μM adenosine because their rates approached the leakage reaction rate. Since the overall rate was limited by the generation of output signal at low adenosine concentrations, the impact of reaction rates between KR and ZR, due to their different toehold lengths, is significantly reduced. In fact, the reaction rates of AT with ZR are slightly faster than AT with KR due to fewer strand displacement steps involved in the 4-way branch migration reaction through **μ** and **μ'** domains which takes place during the reaction between AT and the fuel, affecting the overall reaction rate at 20 μM adenosine and lower. Overall, these results indicate that a longer **μ** domain with higher GC content (28% versus 50%) greatly accelerates the reaction rate of the AT for higher ligand concentrations, but the rates at lower ligand concentrations take a slight reduction.

As shown in Figure 1C, the initial reaction rates exhibited a sigmoidal relationship as a function of adenosine concentration. Such behavior is typical of substrate ligand binding, which originates from the inherent equilibrium reaction between adenosine molecules and the **α** domain of the AT.[8,28] For other studies involving direct aptamer measurement, the aptamer binding affinity (K_d), which depends on aptamer-ligand binding strength and steady-state equilibrium, is determined by the sigmoid half-maximum concentration.[8,28] Since aptamer binding is generally a weak interaction, initial rates quickly decay when the ligand concentration is below the K_d.[8,28] The K_d of the adenosine aptamer sequence used in this work was previously found to be 6 μM, which is near the concentration range found to initiate reaction of the AT and fuel, strongly indicates that the AT and adenosine interaction is the main cause for varied initial reaction rates.[8,28] A maximum reaction rate is reached when all the ATs are bound in steady-state equilibrium to adenosine. Only ATs that are transiently bound to adenosine are available for strand displacement with the fuel, and the population of such ATs increase exponentially with higher adenosine concentrations. Conversely, reactions at lower adenosine concentrations proceed more slowly since fuel strands encounter ATs bound to adenosine molecules at a reduced rate. In the case of the AT reaction in the presence of a reporter, the sigmoidal relation caused by aptamer ligand binding is convoluted by two additional strand displacement steps, and therefore the aptamer binding affinity (K_d) or

effective binding affinity ($K_{d,eff}$) cannot be directly determined. Instead, we define H_{max} as the ligand concentration at half-maximum for initial reaction rate of the AT and use it to compare the performances of AT-reporter reactions. H_{max} should theoretically approach the inherent $K_{d,eff}$ of the aptamer input region (**α + τ'**) when the reaction between the aptamer and the ligand is the rate determining step. We initially tested a range of fuel concentrations from 13 nM – 500 nM, which showed diminishing reaction rate increase above 300 nM [See Supporting Information S1. Optimization of AT-Fuel Concentration Fuel Optimization]. In addition, we optimized the AT reaction conditions with varying buffer salt conditions and performed a selectivity test with two other purine nucleosides – cytidine and uridine - to demonstrate its selectivity [See Supporting Information S2 and S3]. Based on these initial data, we chose to test the AT kinetics with fuel concentrations at 13 nM, which is near the AT concentration of 10 nM, and 300 nM at which the reaction rates leveled off. We observed that the initial reaction rate increased considerably when the fuel concentration increased from 13 nM to 300 nM, which led to the decrease of H_{Max} by a factor of around 4 (4.2 for ZR and 3.9 for KR). The faster reactions can be attributed to the decreased reaction time between the fuel strands and activated ATs, which is significant because the overall reaction rate, hence the detection limit, could be increased without higher adenosine concentration.

One potential downside of increasing the fuel concentration is an increase in the AT reaction network leakage, which is defined as the unintentional reaction of ATs with the fuel without the presence of an input (adenosine).[38] In the case of the AT network, leakage occurs when fuel strands displace the output strand by breathing or fraying of several domains (**β_1**, **β_2**, and **μ**) that leads to branch migration.[38] Such leakage diminishes the sensitivity of the AT device because it is more difficult to differentiate the initial reaction rates at lower adenosine concentrations from the leakage. Although increasing the fuel concentration from 13 to 300 nM nearly doubles the leakage rate, the initial reaction rate at 20 μM adenosine increased by 5-6 times. Moreover, initial reaction rates at lower adenosine concentrations (10 μM and less) were only measurable with 300 nM fuel concentrations since signals at the low concentrations were not detectable when the fuel concentration was 13 nM.

As expected, our results show that the AT reaction is rate limited by two primary factors - (1) the equilibrium reaction rate of the adenosine with the AT and (2) the AT-fuel reaction rate when the fuel concentration is similar to the concentration of AT. The second factor can be mitigated by using excess fuel strands as discussed above. Overall, our ATs were able to successfully accommodate two customized outputs with a limit of detection around 5 μM of adenosine. Therefore, the AT platform demonstrated both the modularity and customizability required for incorporation into feedforward reaction networks. In the next section we demonstrate that the AT can be customized to act as inputs to two amplification reaction networks.

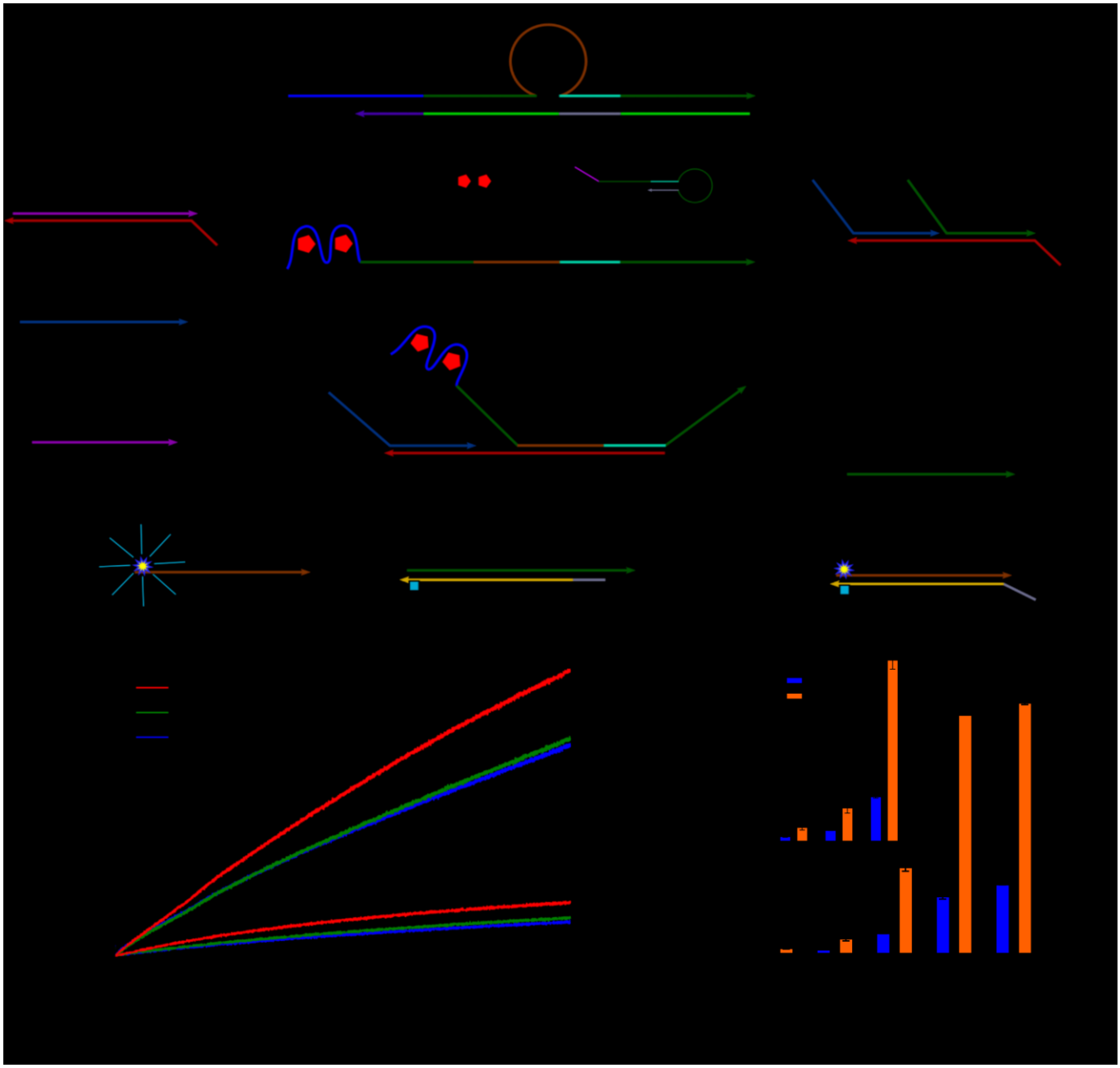

Figure 2: (A) Reaction schematic for AT coupled linear amplification network, AT was redesigned to incorporate 4, 5 domains from 5'-3' ends. (B) Fluorescence intensities of the AT reacted with ZRm (AT+ZRm) compared to AT reacted with ZN (AT+ZN) from 2-20 μM adenosine for 24 hrs (1xTE 25 mM Mg^{2+}) (C) Comparison of leak subtracted differential intensities at 24 hours showing amplification fold for each adenosine concentration from 2-2000 μM.

AT + Entropy-Driven Catalytic Amplification

In order to further validate the modularity of the AT, we redesigned the output strands to initiate DNA reaction networks capable of signal amplification, which is essential for improving signal recognition and the limit of detection.[18,23,24] Catalytic reaction networks, which recycle catalyst strands, are commonly used for non-enzymatic DNA amplification.[23,24] We chose the entropy-driven catalytic network developed by Zhang et al. (ZN) and 3-arm junction catalytic network developed by Kotani et al. (KN) to test such modularity of the AT.[23,24] By

demonstrating the AT's feedforward capability with at least two published reaction networks, the applicability of the ATs to a variety of novel DNA reaction networks could be better evaluated.

As shown in Figure 2A, the integration of AT with ZN (AT-ZN) was accomplished while preserving the original sequences of ZN and by incorporating the initiator sequence into **4** and **5** domains of the aptamer output strand (AO1). Our approach is in contrast to other aptamer amplification networks that modify sequences of the ZN.[18,31] In order to use ZN without such sequence redesign, the **λ** and **μ** domains from the original AT design (Figure 1A) were replaced with **4** and **5** domains of the ZN while keeping other original domains of AT the same. The catalytic network is initiated when the aptamer output strand (AO1) is used as the catalyst binding to the **5'** domain toehold on the ZN substrate (zS1). Upon binding, the **3'** toehold domain of zS1 becomes available when the signal strand (Sig1) is released, allowing for toehold binding of the fuel strand of ZN (zF), which then leads to the release of the output strand (O1) and the aptamer output strand (AO1). The ZR then detects the signal strand (Sig1) and produces a fluorescence signal that can be measured to track the progress of the adenosine sensing reaction. Multiple signal strands (Sig1) can be produced from regenerated aptamer output strand (AO1) and therefore the catalytic network amplifies the AT output signal.

To measure the signal amplification achieved by AT-ZN, a modified reporter (ZRm), whose sequence is presented in the Supporting Information (S4), was designed to directly detect AO1 produced from the reaction of AT-ZN with adenosine by targeting **4** and **5** domains. All amplification experiments were carried out in presence of 300 nM AT-Z fuel since it produced the optimal AT sensitivity in our initial kinetics investigation using ZR. A ratio of 5:1 ZN to AT was used so that the catalytic reaction did not limit the overall reaction rate. The coupled ZN-AT network was continuously monitored for 24 hours to detect adenosine signals (Figure 2B). Adenosine concentrations ranging from 2 μM-2000 μM were detected with the direct reporting method, though overall intensities remained low even after 24 hours. In comparison, the AT-ZN system showed a multifold increase of the leak-subtracted fluorescence intensity compared to the direct reporting method (Figure 2C).

Overall, the AT-ZN system resulted in successful amplification of the reporter fluorescence signal and an enhancement of the adenosine detection limit from 5 to 2 μM (Figure 2C). Compared to the direct reporting network using ZRm, the addition of an amplification network allows the reaction to continue generating signal after the AT has produced an output due to the presence of excess (5:1) ZN. Recycling of the AT output strands (AO1) continued the amplification reaction, leading to higher final fluorescence intensities compared with the direct reporting network that uses ZRm as the reporter. The 5:1 substrate to AT ratio allowed the system to amplify low adenosine concentrations by a factor of about 3-4 fold when compared to AT without an amplification network (Figure 2C). While an adenosine signal was successfully amplified, leakage from the AT network was also amplified in the process. Thus, minimization of the AT network leakage is an important consideration in improving device performance, especially when coupled to an amplifier. Similarly, the catalytic network in use must not introduce extraneous leakage to avoid signal interference.

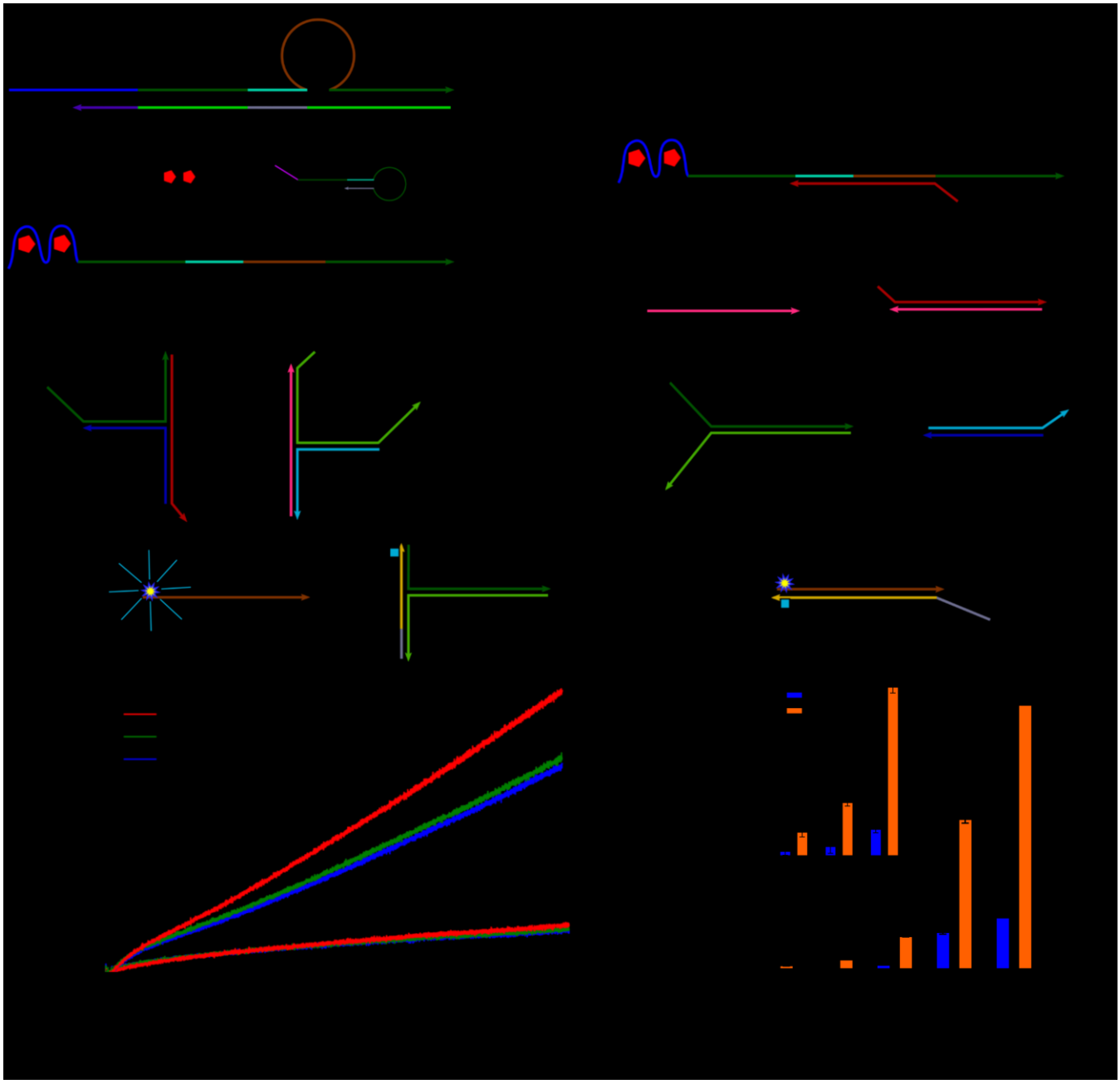

Figure 3: (A) Reaction schematic for AT coupled 3-arm amplification network, AT was redesigned to incorporate 1, c, a domains from 5'-3' ends. Note: the AT μ domain has been moved to preserve 5'-3' of the amplifier RN (B) Fluorescence intensities of the AT reacted with KRm (AT+KRm) compared to AT reacted with KN (AT+KN) from 2-20 μM adenosine for 24 hrs (1xTE 25 mM Mg^{2+}) C) Comparison of leak subtracted differential intensities at 24 hours showing amplification fold for each adenosine concentration from 2-2000 μM.

AT + 3-Arm Catalytic Amplification

The second catalytic network by Kotani et al. (KN), which utilizes 3-arm substrates, was integrated with the AT to create AT-KN. One difference between AT-ZN and AT-KN is how the catalyst is recycled. AT-ZN reuses the Aptamer Output strand (AO1 in Figure 2A) for catalytic amplification, while KN outputs a new catalyst strand (C1) that acts as the catalyst for multiple cycles (Figure 3A). This difference in the design of AT-

KN plays a role in improved amplification compared to ZN, since the initial AT output strands (AO1) contain extraneous domains that could add steric hindrance to the system. The KN has been shown to have a rate comparable to ZN having rate constants within an order of magnitude of each other.[24] Another important difference between KN and ZN is that KN was shown to reduce the rate of catalytic network leakage, which requires a slower 4-arm branch migration.[24] Reduction in the leakage of the amplifying network translates to improvements in network stability and lower detection limit of the AT network in principle.

Integrating the AT with the KN required slight modification of the AT network design since the location of the toehold domain (**1** domain) is on the 5' end of its input compared to ZN whose toehold domain (domain **5**) is on the 3' end of the input (Figure 3A). To accommodate such differences, the **μ** and **μ'** domains simply have been moved to the opposite side of the **λ** domain, which further validates the sequence modularity and customizability of the AT design since other known feed-forward networks may require 3' to 5' reversal for function. In addition to changing the location of the toehold (domain **1**), **c** and **a** domains were changed so that the probe strand could initiate the KN. The operation of AT-KN is initiated by the strand displacement between the aptamer output strand (AO2) and Substrate 1 (S1) which form Product 4 (P4). The remainder of S1 then reacts with Substrate 2 (S2) to generate Product 2 (P2), Product 3 (P3), and a catalyst strand (C1). C1 strand then reacts with S1 and generate Product 1 (P1) thus initiating another cycle. Since the C1 strand is regenerated for each subsequent reaction cycle, the system continues to operate as long as the S1 and S2 strands are available. The P2 strand reacts with the reporter (KR) to generate fluorescence signals that can be continuously monitored.

Similar to AT-ZN system and the use of ZRm, a modified reporter (KRm), whose sequence is presented in the Supporting Information (S4), was designed to directly detect AO2 produced from the reaction of AT-ZN with adenosine by targeting **1**, **c**, and **a** domains. As with the AT-ZN system, AT-KN substrates (S1 and S2) where reacted at 5:1 substrate to AT with excess AT-K fuel at 300 nM. After reacting for 24 hours, the AT-KN was able to achieve a limit of detection of 2 μM, whereas the AT-KRm was able to detect only 20 μM. A net amplification of about 4-6 times was achieved by the KN system comparing the leak subtracted signals for AT-KRm and AT-KN (Figure 3C). Specifically, the fluorescence signal with 2 μM adenosine was amplified by around 4.6 times while there was little to detectable signal exhibited by the AT-KRm control. This result confirms that the KN can effectively boost even relatively weak adenosine signals into a detectable range. This may be partly due to the AT-KN's ability to produce a smaller and more reactive catalyst strand, as well as smaller leakage signal produced the KN.

The adenosine detection tests with the feed-forward network reactions (AT-ZN and AT-KN) clearly demonstrate both modularity and customizability of the AT to effectively trigger downstream amplification networks. In both cases, redesigned AT outputs produced catalytic inputs to their targeted amplification reaction networks (ZN and KN) with minimal modification of the AT without any need for redesign of the original networks. One difference between the AT-ZN and AT-KN systems is the role of AT aptamer output strands (AO1 and AO2) in their respective amplification networks. AO1 acts as the catalyst for ZN for every catalytic cycle whereas AO2 is involved only in the initial catalytic cycle of KN, which contributes to greater amplification of AT-KN. These different operation mechanisms, however, are a function of the design of original network. ATs integrated with ZN components (AT-ZN and AT-ZRm) showed a greater initial reaction rate than AT-KN and AT-KRm (Figures 2B and 3B), which could be attributed to ZN and ZRm's shorter duplex domains (**4** and **4'**, 16 nts) of the substrate compared to such domains in KN and KRm (**a c** and **a' c',** 45 nts). The AT-KN and AT-KRm branch migration domains were ~3 times longer, which contributed to their ~ 4 times smaller fluorescence intensity when compared with the AT-ZN and AT-ZRm systems.[39] Despite slower reaction triggered by AO2, the AT-KN showed ~ 52%, 89%, and 52% greater amplification compared to AT-ZN for low adenosine concentrations, 2 μM, 5 μM and 20 μM respectively demonstrating that the KN is a more effective amplification network for our ATs due to its lower leakage rate and its smaller catalyst strand.

In comparison to published feed-forward adenosine detection network that also uses the entropy-driven catalytic network by Zhang et al. and has been shown to have a detection limit of 20 nM adenosine, the sensitivity and detection limits of our feed-forward AT networks requires further improvement and optimization.[23,31] A thorough investigation of network leakage mechanisms and design alterations to the AT could help improve the sensitivity of the adenosine sensor, especially when coupled to a catalytic network for amplification of the AT output. Regardless of these limitations, our feed-forward AT network is a more versatile platform based on its customizability that allows the sequence and domain designs for previously optimized catalytic amplification networks to be incorporated as demonstrated with ZN and KN. Future study of the AT should aim to test the modularity of the **α** input domain with different aptamers to understand its applicability to detect other analytes. Understanding the interaction between the **τ'** domain and other aptamer sequences poses a potential challenge since many structure-switching mechanisms are not yet well understood. Hence, a thorough study of the **τ'** domain's interactions with other aptamers and their respective secondary structures is vital for expanding the usefulness of the AT network. Additionally, rational design and testing of the **τ'** domain will provide a greater understanding of how decreasing the $K_{d,eff}$ of the AT might increase the downstream catalytic amplification and improve sensitivity. Multiplexed AT systems capable of detecting many ligands simultaneously with targeted and customizable AT networks could allow development of more sophisticated biosensing tools, as the understanding of aptamer structure-switching mechanisms by the community advances.

Conclusions

We demonstrated that the aptamer transducer network that contains independent aptamer sensing and downstream signal domains can function as a modular aptamer reaction network, which can produce customizable DNA outputs. Our aptamer transducer successfully detected adenosine and produced four different output strands that were integrated into different reporting and amplification networks without any modifications to the downstream reaction networks. The limit of adenosine detection was limited by the $K_{d,eff}$ of the aptamer input domain. Integration of aptamer transducers with amplifications networks resulted in multifold increase of florescence signals indicating successful downstream reactions and enhanced detection limits.

Overall, our aptamer transducer framework was successfully designed as a novel non-enzymatic modular aptamer sensor unit that can be incorporated into many other reaction networks for direct target detection. Our work with the aptamer transducer framework provides a good platform for the investigation of more general and modular aptamer reaction network systems that could lead to more sensitive and universal biosensing systems.

Experimental

DNA Preparation

DNA strands were purchased from Integrated DNA Technologies (IDT). [See Supporting Information S4. Strand Sequences for Aptamer Transducer and Catalytic Amplification Networks for a list of base sequences.] Prior to ordering, validation of the correct secondary structures was tested using NUPACK.[40] [See Supporting Information S5. NUPACK Secondary Structures of ATs] Dye- or quencher-labeled strands or those longer than 80 nucleotides (nt) were purified by high performance liquid chromatography (HPLC) by IDT. Dye strands were modified on the 5' end with Tetrachlorofluorescein (TET) and quencher strands were modified on the 3' end with Iowa Black Quencher (IABkFQ, IDT). Upon receiving, strands were re-suspended until they reached ~100 μM in 1×TE buffer (Sigma-Aldrich). AT, catalytic substrates, and reporter complexes were stoichiometrically mixed in 1×TE buffer with 12.5 mM $MgCl_2$ (1×TE Mg^{2+}). Prior to annealing and PAGE purification, samples were diluted to 20 μM in 1×TAE buffer. All dsDNA complexes were annealed at 90 ºC for 5 minutes and then cooled to 20 ºC at a rate of 5 ºC per minute to room temperature.

DNA Purification

DNA strands were purified by PAGE gel electrophoresis prior to use. 1.5 mm thick 10 cm × 10 cm non-denatured 10% gels for PAGE (acrylamide:bis = 29:1) were prepared with 1×TAE buffer. A loading buffer was prepared by mixing a 50:50 solution containing ficcol and bromophenol blue. Previously annealed samples were mixed with loading buffer (4:1) prior to being loaded into gel wells in 25 μL increments. Electrophoresis was carried out at 150 V, 100 mA, 20 W, for 2.5 hrs. Bands cut from each gel contained the purified complex which were eluted in ~ 500 μL 1×TE buffer with 25 mM $MgCl_2$. After 48 hours of elution, purified DNA complexes were transferred to new low binding Eppendorf Tubes.

Kinetics Experiments

Samples were vortexed and centrifuged before quantification using a NanoDrop One (Thermo Scientific) at 260 nm. Extinction coefficients, provide by IDT, were used to determine the DNA complex concentrations prior to mixing the reactants. Purified and diluted DNA samples were reacted in stoichiometric quantities. Reaction kinetics were measured with Varian or Agilent Cary Eclipse fluorometers using transparent disposable PMMA cuvettes (excitation λ=522 nm, emission λ=539 nm, 25 ºC).

Acknowledgments

We thank members of the Boise State Nanoscale Materials and Device group for valuable assistance with this work. We also thank Boise State University Micron School of Materials Science & Engineering Department for supporting this work. This work was supported in part by grant no. 1706065 from the National Science Foundation.

Supporting Information

The Supporting information is available free of charge on the ACS Publications website at DOI: XXX:

Strand sequences, NUPACK secondary structures results, optimization of AT-Fuel concentrations, optimization of buffer salt concentrations, and selectivity of the AT targeting adenosine are provided.

Author Information

Tim Hachigian: timhachigian@u.boisestate.edu
Drew Lysne: drewlysne@u.boisestate.edu
Elton Graugnard: eltongraugnard@boisestate.edu
Jeunghoon Lee: jeunghoonlee@boisestate.edu

References

(1) Ellington, A. D.; Szostak, J. W. In Vitro Selection of RNA Molecules That Bind Specific Ligands. *Nature* **1990**, *346* (6287), 818–822. https://doi.org/10.1038/346818a0.

(2) Huizenga, D. E.; Szostak, J. W. A DNA Aptamer That Binds Adenosine and ATP. *Biochemistry* **1995**, *34* (2), 656–665. https://doi.org/10.1021/bi00002a033.

(3) Tuerk, C.; Gold, L. Systematic Evolution of Ligands by Exponential Enrichment: RNA Ligands to Bacteriophage T4 DNA Polymerase. *Science* **1990**, *249* (4968), 505–510. https://doi.org/10.1126/science.2200121.

(4) Luo, Y. Functional Nucleic Acid Biosensors for Small Molecules. In *Functional Nucleic Acid Based Biosensors for Food Safety Detection*; Luo, Y., Ed.; Springer Singapore: Singapore, 2018; pp 249–306. https://doi.org/10.1007/978-981-10-8219-1_10.

(5) Shaban, S. M.; Kim, D.-H. Recent Advances in Aptamer Sensors. *Sensors* **2021**, *21* (3). https://doi.org/10.3390/s21030979.

(6) Yu, H.; Alkhamis, O.; Canoura, J.; Liu, Y.; Xiao, Y. Advances and Challenges in Small-Molecule DNA Aptamer Isolation, Characterization, and Sensor Development. *Angew. Chem. Int. Ed.* **2021**, *60* (31), 16800–16823. https://doi.org/10.1002/anie.202008663.

(7) Munzar JD; Ng A; Juncker D. Duplexed Aptamers: History, Design, Theory, and Application to Biosensing. *Chem. Soc. Rev.* **2019**, *48* (5), 1390–1419. https://doi.org/10.1039/c8cs00880a.

(8) Munzar, J. D.; Ng, A.; Juncker, D. Comprehensive Profiling of the Ligand Binding Landscapes of Duplexed Aptamer Families Reveals Widespread Induced Fit. *Nat. Commun.* **2018**, *9* (1), 343. https://doi.org/10.1038/s41467-017-02556-3.

(9) Monserud, J. H.; Macri, K. M.; Schwartz, D. K. Toehold-Mediated Displacement of an Adenosine-Binding Aptamer from a DNA Duplex by Its Ligand. *Angew. Chem. Int. Ed.* **2016**, *55* (44), 13710–13713. https://doi.org/10.1002/anie.201603458.

(10) Carrasquilla, C.; Li, Y.; Brennan, J. D. Surface Immobilization of Structure-Switching DNA Aptamers on Macroporous Sol-Gel-Derived Films for Solid-Phase Biosensing Applications. *Anal. Chem.* **2011**, *83* (3), 957–965. https://doi.org/10.1021/ac102679r.

(11) Nutiu, R.; Li, Y. Structure-Switching Signaling Aptamers: Transducing Molecular Recognition into Fluorescence Signaling. *Chem. - Eur. J.* **2004**, *10* (8), 1868–1876. https://doi.org/10.1002/chem.200305470.

(12) Nutiu, R.; Li, Y. Structure-Switching Signaling Aptamers. *J. Am. Chem. Soc.* **2003**, *125* (16), 4771–4778. https://doi.org/10.1021/ja028962o.

(13) Shlyahovsky, B.; Li, D.; Weizmann, Y.; Nowarski, R.; Kotler, M.; Willner, I. Spotlighting of Cocaine by an Autonomous Aptamer-Based Machine. *J. Am. Chem. Soc.* **2007**, *129* (13), 3814–3815. https://doi.org/10.1021/ja069291n.

(14) Meng, C.; Dai, Z.; Guo, W.; Chu, Y.; Chen, G. Selective and Sensitive Fluorescence Aptamer Biosensors of Adenosine Triphosphate. *Nanomater. Nanotechnol.* **2016**, *6*, 33. https://doi.org/10.5772/63985.

(15) Li, B.; Ellington, A. D.; Chen, X. Rational, Modular Adaptation of Enzyme-Free DNA Circuits to Multiple Detection Methods. *Nucleic Acids Res.* **2011**, *39* (16), e110. https://doi.org/10.1093/nar/gkr504.

(16) Ravan, H. Implementing a Two-Layer Feed-Forward Catalytic DNA Circuit for Enzyme-Free and Colorimetric Detection of Nucleic Acids. *Anal. Chim. Acta* **2016**, *910*, 68–74. https://doi.org/10.1016/j.aca.2016.01.013.

(17) Zhou, Z.; Du, Y.; Dong, S. Double-Strand DNA-Templated Formation of Copper Nanoparticles as Fluorescent Probe for Label-Free Aptamer Sensor. *Anal. Chem.* **2011**, *83* (13), 5122–5127. https://doi.org/10.1021/ac200120g.

(18) Cheng, S.; Zheng, B.; Wang, M.; Zhao, Q.; Lam, M. H.; Ge, X. Determination of Adenosine Triphosphate by a Target Inhibited Catalytic Cycle Based on a Strand Displacement Reaction. *Anal. Lett.* **2014**, *47* (3), 478–491. https://doi.org/10.1080/00032719.2013.841179.

(19) Wang, J.; Munir, A.; Zhou, S. H. Au NPs-Aptamer Conjugates as a Powerful Competitive Reagent for Ultrasensitive Detection of Small Molecules by Surface Plasmon Resonance Spectroscopy. *Talanta TA - TT* - **2009**, *79* (1), 72–76. https://doi.org/10.1016/j.talanta.2009.03.003.
(20) Meng, H.-M.; Liu, H.; Kuai, H.; Peng, R.; Mo, L.; Zhang, X.-B. Aptamer-Integrated DNA Nanostructures for Biosensing, Bioimaging and Cancer Therapy. *Chem. Soc. Rev.* **2016**, *45* (9), 2583–2602. https://doi.org/10.1039/C5CS00645G.
(21) Zhu, J.; Zhang, L.; Zhou, Z.; Dong, S.; Wang, E. Aptamer-Based Sensing Platform Using Three-Way DNA Junction-Driven Strand Displacement and Its Application in DNA Logic Circuit. *Anal. Chem.* **2014**, *86* (1), 312–316. https://doi.org/10.1021/ac403235y.
(22) Zheng, D.; Seferos, D. S.; Giljohann, D. A.; Patel, P. C.; Mirkin, C. A. Aptamer Nano-Flares for Molecular Detection in Living Cells. *Nano Lett.* **2009**, *9* (9), 3258–3261. https://doi.org/10.1021/nl901517b.
(23) Zhang, D. Y.; Turberfield, A. J.; Yurke, B.; Winfree, E. Engineering Entropy-Driven Reactions and Networks Catalyzed by DNA. *Science* **2007**, *318* (5853), 1121–1125. https://doi.org/10.1126/science.1148532.
(24) Kotani, S.; Hughes, W. L. Multi-Arm Junctions for Dynamic DNA Nanotechnology. *J. Am. Chem. Soc.* **2017**, *139* (18), 6363–6368. https://doi.org/10.1021/jacs.7b00530.
(25) Xiao, Y.; Piorek, B. D.; Plaxco, K. W.; Heeger, A. J. A Reagentless Signal-on Architecture for Electronic, Aptamer-Based Sensors via Target-Induced Strand Displacement. *J. Am. Chem. Soc.* **2005**, *127* (51), 17990–17991. https://doi.org/10.1021/ja056555h.
(26) Fu, B.; CAo, J.; Wang, L.; Jiang, W. A Novel Enzyme-Free and Label-Free Fluorescence Aptasensor for Amplified Detection of Adenosine. *Biosens. Bioelectron.* **2013**, *44* (1), 52–56. https://doi.org/10.1016/j.bios.2012.12.059.
(27) Wang, K.; He, M.; Zhai, F.; Chen, R.; Yu, Y. A Label-Free and Enzyme-Free Ratiometric Fluorescence Biosensor for Sensitive Detection of Carcinoembryonic Antigen Based on Target-Aptamer Complex Recycling Amplification. *Sens. Actuators B Chem.* **2017**, *253*, 893–899. https://doi.org/10.1016/j.snb.2017.07.047.
(28) Armstrong, R. E.; Strouse, G. F. Rationally Manipulating Aptamer Binding Affinities in a Stem-Loop Molecular Beacon. *Bioconjug. Chem.* **2014**, *25* (10), 1769–1776. https://doi.org/10.1021/bc500286r.
(29) Jung, C.; Ellington, A. D. Diagnostic Applications of Nucleic Acid Circuits. *Acc. Chem. Res.* **2014**, *47* (6), 1825–1835. https://doi.org/10.1021/ar500059c.
(30) Zhang, D. Y.; Seelig, G. Dynamic DNA Nanotechnology Using Strand-Displacement Reactions. *Nat. Chem.* **2011**, *3* (2), 103–113. https://doi.org/10.1038/nchem.957.
(31) Cheng, S.; Zheng, B.; Wang, M.; Ge, X.; Lam, M. H. A Target-Triggered Strand Displacement Reaction Cycle: The Design and Application in Adenosine Triphosphate Sensing. *Anal. Biochem.* **2014**, *446* (1), 69–75. https://doi.org/10.1016/j.ab.2013.10.021.
(32) Cho, E. J.; Yang, L.; Levy, M.; Ellington, A. D. Using a Deoxyribozyme Ligase and Rolling Circle Amplification to Detect a Non-Nucleic Acid Analyte, ATP. *J. Am. Chem. Soc.* **2005**, *127* (7), 2022–2023. https://doi.org/10.1021/ja043490u.
(33) Liu, J.; Lu, Y. Non-Base Pairing DNA Provides a New Dimension for Controlling Aptamer-Linked Nanoparticles and Sensors. *J. Am. Chem. Soc.* **2007**, *129* (27), 8634–8643. https://doi.org/10.1021/ja072075+.
(34) Zhang, Z.; Oni, O.; Liu, J. New Insights into a Classic Aptamer: Binding Sites, Cooperativity and More Sensitive Adenosine Detection. *Nucleic Acids Res.* **2017**, *45* (13), 7593–7601. https://doi.org/10.1093/nar/gkx517.
(35) Nakamura, I.; Shi, A.-C.; Nutiu, R.; Yu, J.; Li, Y. Kinetics of Signaling-DNA-Aptamer-ATP Binding. *Phys. Rev. E Stat. Nonlin. Soft Matter Phys.* **2009**, *79* (3), 31906. https://doi.org/10.1103/PhysRevE.79.031906.
(36) Lee, J.; Jeon, C. H.; Ahn, S. J.; Ha, T. H. Highly Stable Colorimetric Aptamer Sensors for Detection of Ochratoxin A through Optimizing the Sequence with the Covalent Conjugation of Hemin. *The Analyst* **2014**, *139* (7), 1622–1627. https://doi.org/10.1039/c3an01639k.

(37) Dunn, K. E.; Trefzer, M. A.; Johnson, S.; Tyrrell, A. M. Investigating the Dynamics of Surface-Immobilized DNA Nanomachines. *Sci. Rep.* **2016**, *6*, 29581. https://doi.org/10.1038/srep29581.
(38) Lysne, D.; Jones, K.; Stosius, A.; Hachigian, T.; Lee, J.; Graugnard, E. Availability-Driven Design of Hairpin Fuels and Small Interfering Strands for Leakage Reduction in Autocatalytic Networks. *J. Phys. Chem. B* **2020**, *124* (16), 3326–3335. https://doi.org/10.1021/acs.jpcb.0c01229.
(39) Srinivas, N.; Ouldridge, T. E.; Sulc, P.; Schaeffer, J. M.; Yurke, B.; AA, L.; JP, D.; Winfree, E. On the Biophysics and Kinetics of Toehold-Mediated DNA Strand Displacement. *Nucleic Acids Res.* **2013**, *41* (22), 10641–10658. https://doi.org/10.1093/nar/gkt801.
(40) Zadeh, J. N.; Steenberg, C. D.; Bois, J. S.; Wolfe, B. R.; Pierce, M. B.; Khan, A. R.; Dirks, R. M.; Pierce, N. A. NUPACK: Analysis and Design of Nucleic Acid Systems. *J. Comput. Chem.* **2011**, *32* (1), 170–173. https://doi.org/10.1002/jcc.21596.

TOC Graphic:

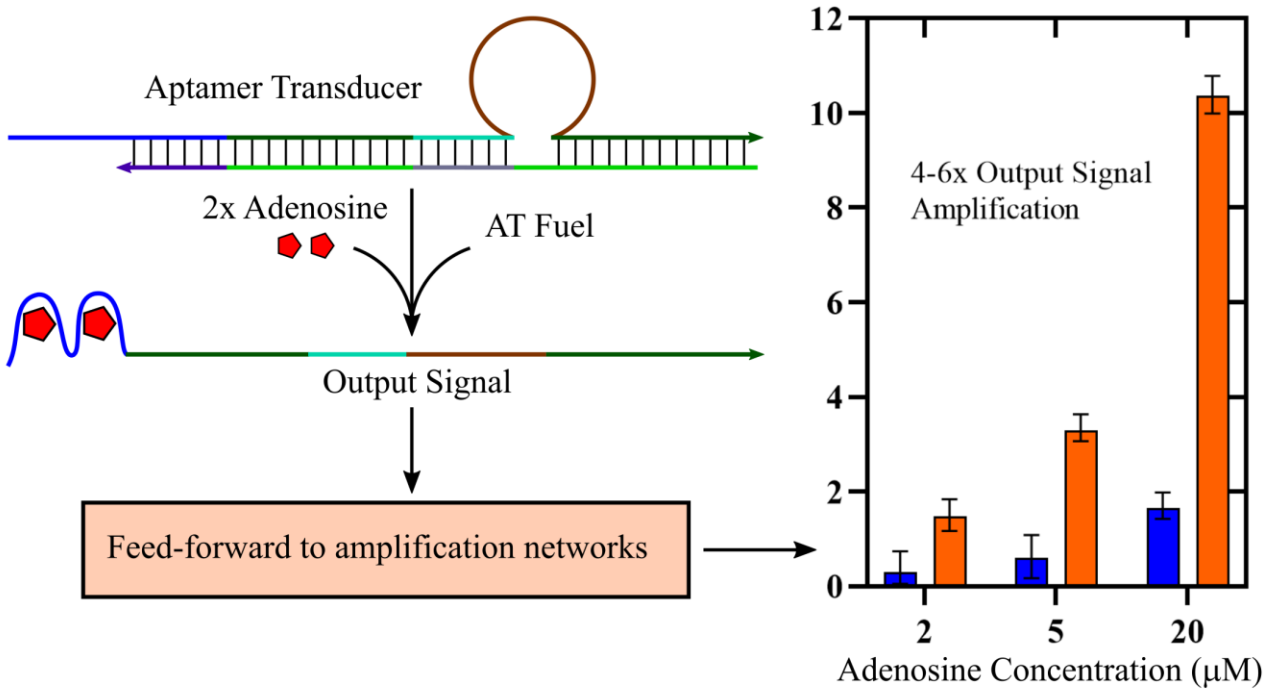
Aptamer Transducer
2x Adenosine
AT Fuel
Output Signal
Feed-forward to amplification networks
4-6x Output Signal Amplification
12
10
8
6
4
2
0
2
5
20
Adenosine Concentration (μM)